Electronic Supplementary Material (ESI) for Journal of Materials Chemistry C.
This journal is © The Royal Society of Chemistry 2021

Supplementary Information

In-situ growth of polyoxometalate in COF for trace monitoring Ag^+ and hepatocellular carcinoma biomarker via dual responsive strategy

Jinmin Wang,[a] Xin Xu[a], Limin Zhao,*[,b] and Bing Yan*[,a,b]

[a] Shanghai Key Lab of Chemical Assessment and Sustainability, School of Chemical Science and Engineering, Tongji University, Shanghai 200092, China

[b] School of Materials Science and Engineering, Liaocheng University, Liaocheng 252059, China

* Corresponding author: byan@tongji.edu.cn

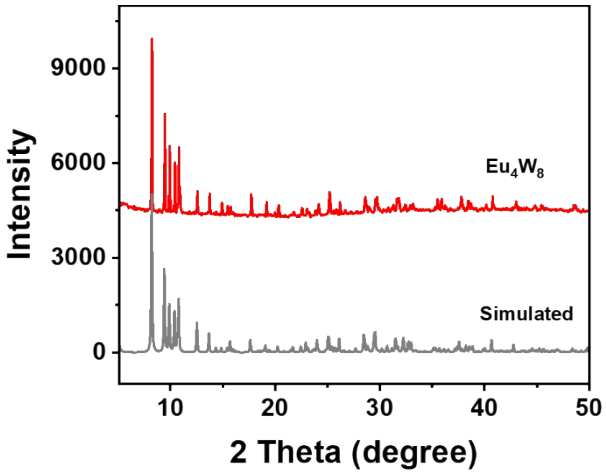

Figure S1. PXRD patterns of Eu_4W_8.

Table S1. Weight percentage of all elements in Eu_4W_8@EB-TFP determined by EDX.

Element	Percentage by weight
C	58.88
N	7.61
O	11.64
Na	2.24
Cl	2.44
Br	0.72
Eu	1.00
W	15.48

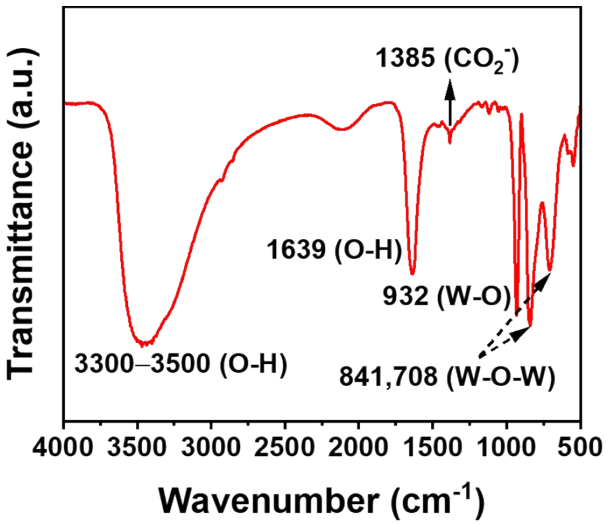

Figure S2. FTIR spectrum of Eu_4W_8.

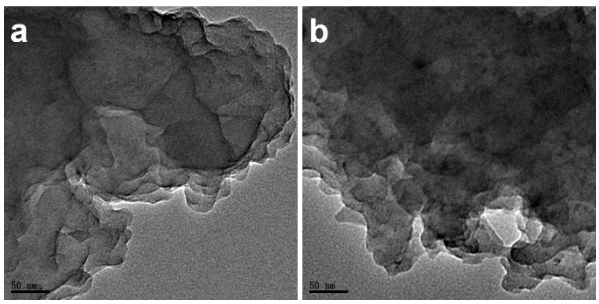

Figure S3. TEM images of EB-TFP (a) and Eu_4W_8@EB-TFP (b).

Table S2. The BET surface area and pore volume of EB-TFP and Eu_4W_8@EB-TFP.

Sample	BET surface area ($m^2 g^{-1}$)	Pore volume ($cm^3 g^{-1}$)
COF EB-TFP	713.54	0.27
Eu_4W_8@EB-TFP (2 days prepared)	422.78	0.14
Eu_4W_8@EB-TFP (4 days prepared)	11.12	0.06

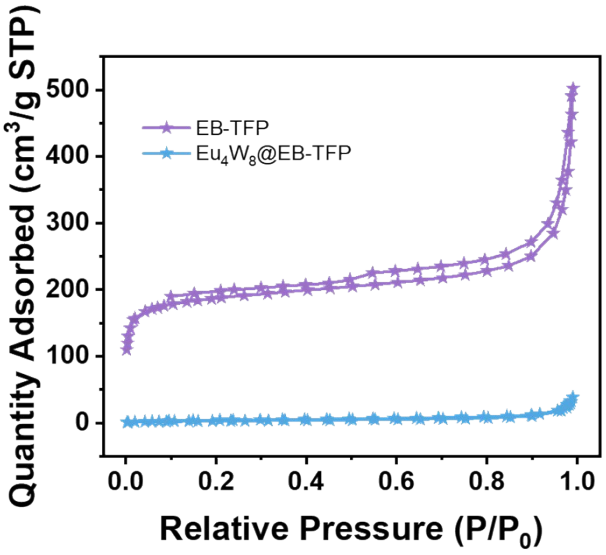

Figure S4. The N_2 adsorption-desorption isotherms of EB-TFP and Eu_4W_8@EB-TFP after heat-treatment.

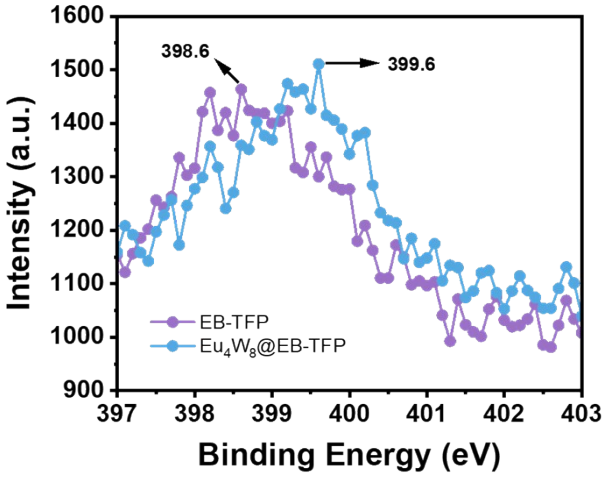

Figure S5. XPS spectra of EB-TFP and Eu_4W_8@EB-TFP for N 1s electrons.

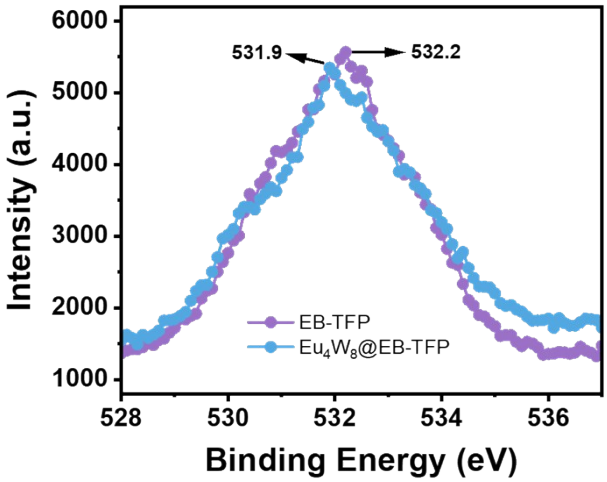

Figure S6. XPS spectra of EB-TFP and Eu_4W_8@EB-TFP for O 1s electrons.

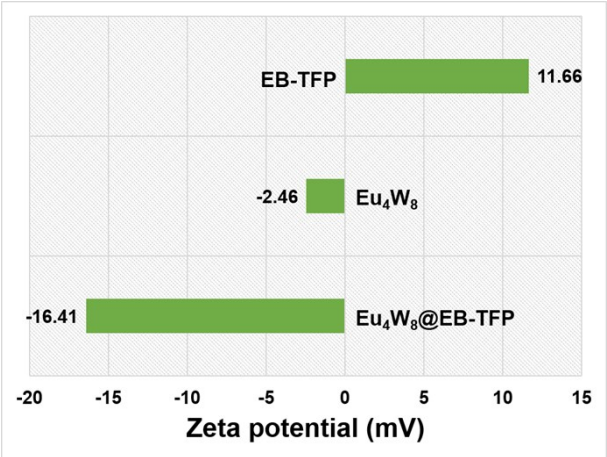

Figure S7. ζ-Potential analysis of EB-TFP, Eu_4W_8 and Eu_4W_8@EB-TFP suspensions.

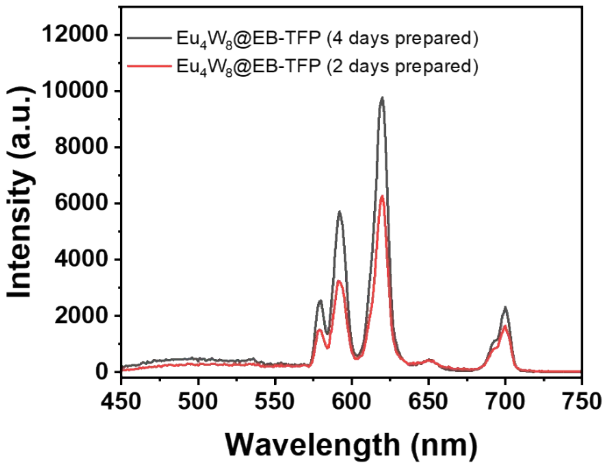

Figure S8. Luminescence spectra (λ_{ex} = 284 nm) of Eu_4W_8@EB-TFP with different growth times.

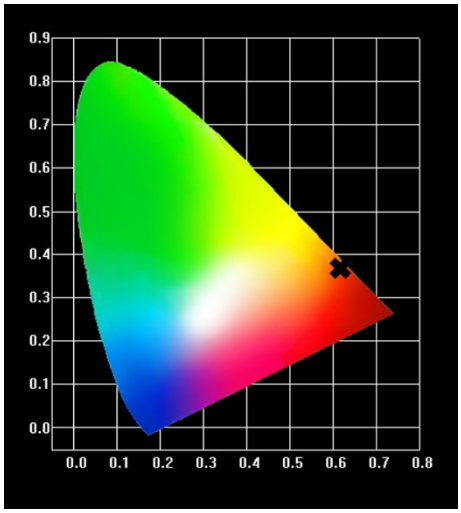

Figure S9. CIE coordinate of Eu_4W_8@EB-TFP suspension.

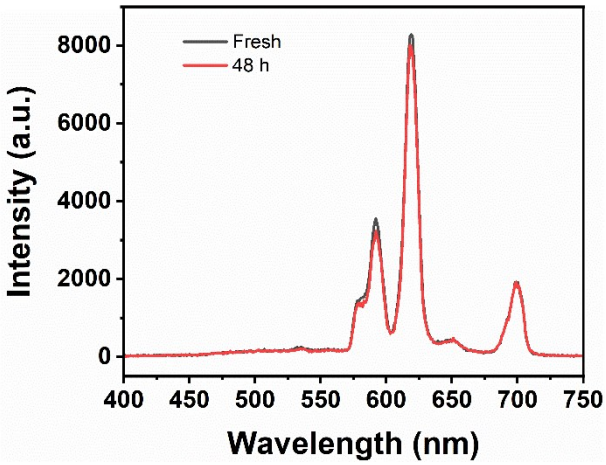

Figure S10. Luminescence spectra (λ_{ex} = 284 nm) of Eu_4W_8@EB-TFP before and after

storage in water for 48 h.

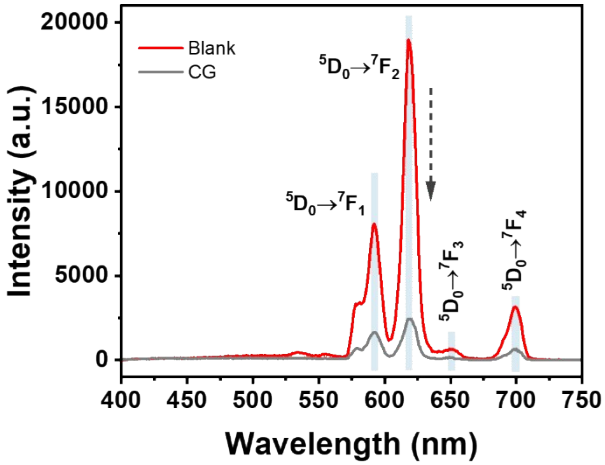

Figure S11. Luminescence spectra (λ_{ex} = 284 nm) of Eu_4W_8@EB-TFP before and after the addition of CG. The concentration of CG was 10^{-3} M.

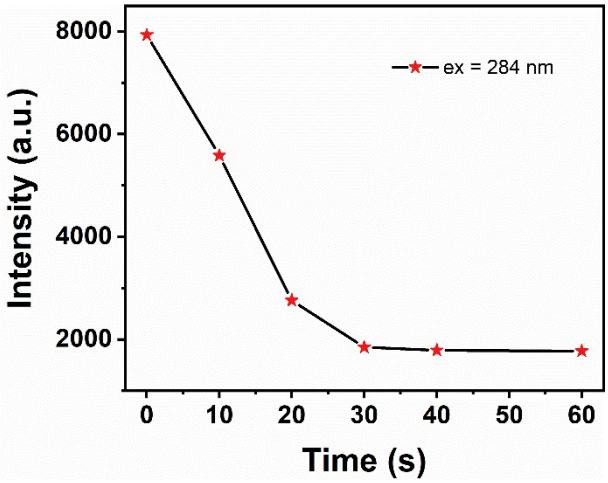

Figure S12. Time-dependent luminescence intensity of Eu_4W_8@EB-TFP at 615 nm with CG, the concentration of CG was 10^{-3} M (λ_{ex} = 284 nm).

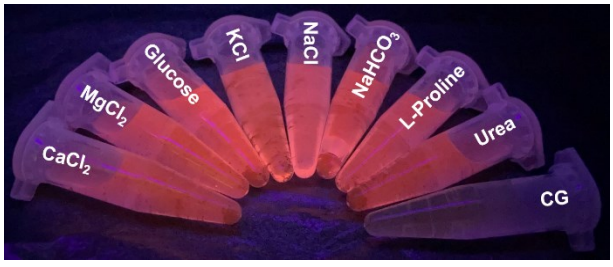

Figure S13. Photos of Eu_4W_8@EB-TFP with CG or other serum components under 254

nm UV-light irradiation. The concentrations of CG and serum components were 10^{-3} M.

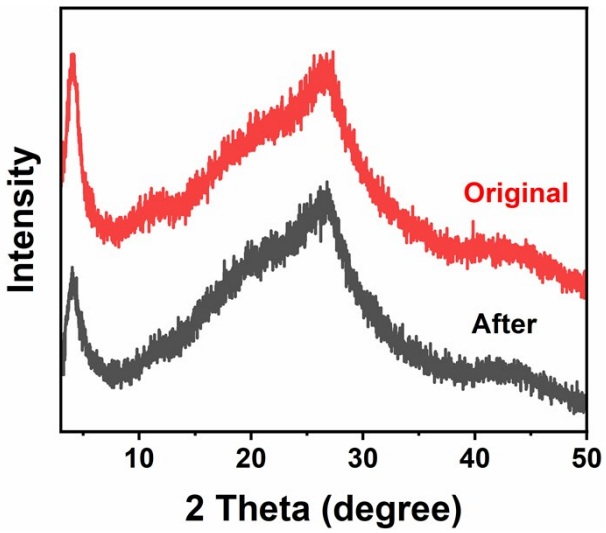

Figure S14. PXRD patterns of Eu_4W_8@EB-TFP before and after sensing CG.

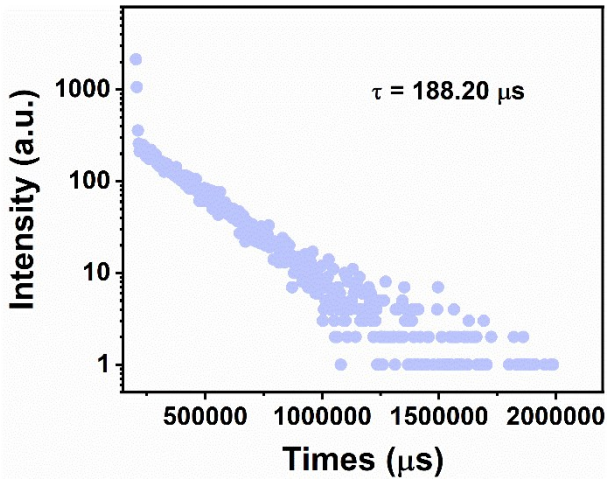

Figure S15. Lifetime decay curve of Eu_4W_8@EB-TFP added with 10^{-3} M CG (λ_{ex} = 284 nm, λ_{em} = 615 nm).

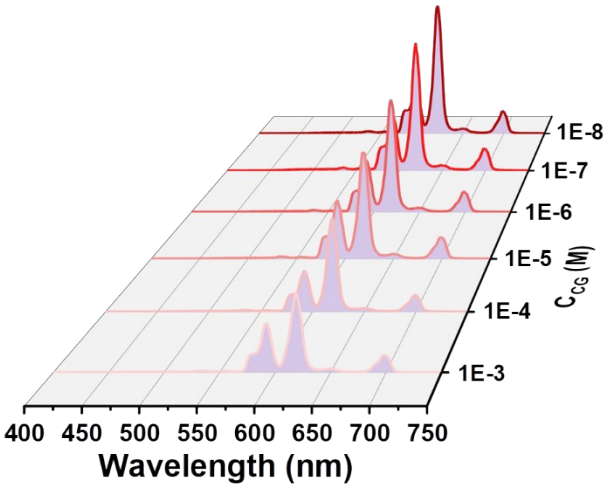

Figure S16. Luminescence spectra of Eu_4W_8@EB-TFP added CG in serum system with different concentrations (10^{-8}–10^{-3} M).

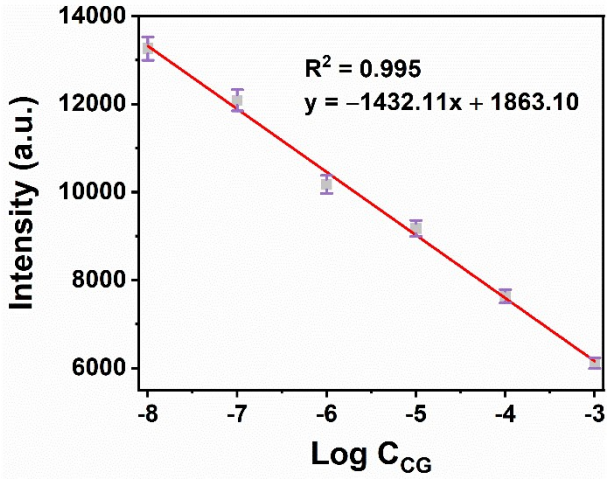

Figure S17. Calibration curves of Eu_4W_8@EB-TFP added CG in serum system with different concentrations (10^{-8}–10^{-3} M).

Table S3. Comparison of EB-TFP@Eu_4W_8 with other CG sensors (limit of detection: LOD).[1–4]

Analytical method	Detection range	LOD	Detection environment	Reference
Enzyme-linked immunosorbent assay	0.02–0.18 μg mL $^{-1}$	0.06 μg mL $^{-1}$	Buffer solution	1
Fluorescence polarization immunoassay	163.1–2853.8 ng mL^{-1}	50.9 ng mL^{-1}	Serum	2
Enzyme multiplied immunoassay technique	0.6–40 μg mL^{-1}	0.79 μg mL^{-1}	Serum	3
Enzyme multiplied immunoassay technique	0–40 μg mL^{-1}	0.4 μg mL^{-1}	Buffer solution	4
Fluorescence analysis	0.005–465 μg mL^{-1}	0.043 μg mL^{-1}	Serum	This work

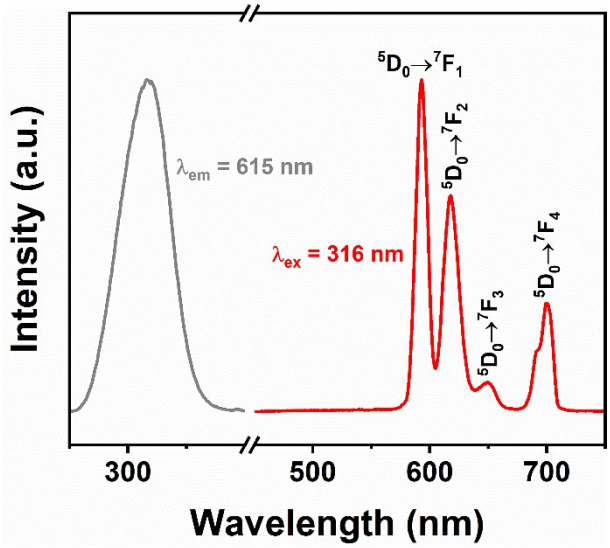

Figure S18. Excitation and emission spectra of Eu_4W_8@EB-TFP added Ag^+ in aqueous solution.

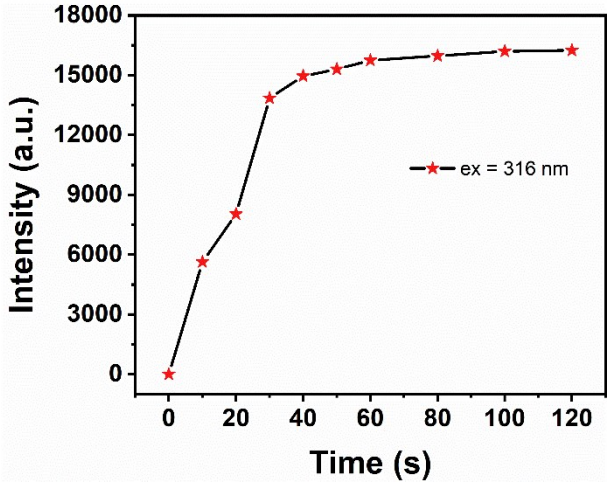

Figure S19. Time-dependent luminescence intensity of Eu_4W_8@EB-TFP at 615 nm with Ag^+, the concentration of Ag^+ was 10^{-3} M (λ_{ex} = 316 nm).

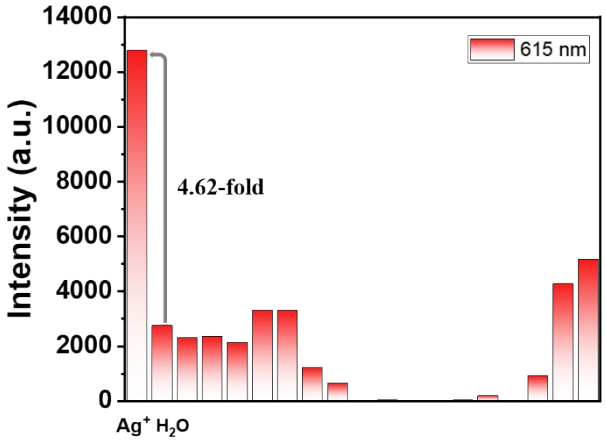

Figure S20. Selectivity of Eu_4W_8 with different metal ions (λ_{ex} = 316 nm) (1–19: Ag^+, H_2O, Li^+, Na^+, K^+, Mg^{2+}, Ca^{2+}, Ba^{2+}, Al^{3+}, Cr^{3+}, Mn^{2+}, Fe^{2+}, Fe^{3+}, Co^{2+}, Ni^{2+}, Cu^{2+}, Zn^{2+}, Cd^{2+}, Pb^{2+}). The concentrations of metal ions were 10^{-3} M.

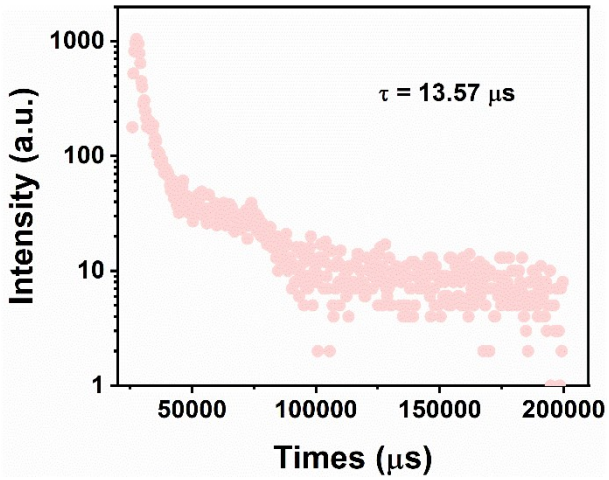

Figure S21. Lifetime decay curve of Eu_4W_8@EB-TFP (λ_{ex} = 316 nm, λ_{em} = 615 nm).

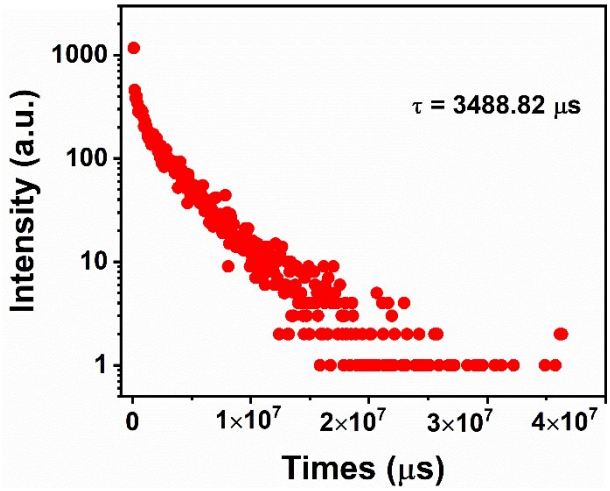

Figure S22. Lifetime decay curve of Eu_4W_8@EB-TFP added with 10^{-3} M Ag^+ (λ_{ex} = 316 nm, λ_{em} = 615 nm).

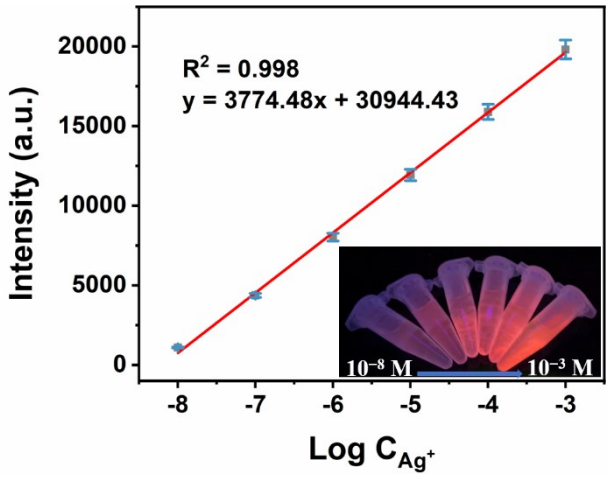

Figure S23. Calibration curves of Eu_4W_8@EB-TFP added Ag^+ in aqueous solution with different concentrations (10^{-8}–10^{-3} M). Inset: The corresponding photos under 310 nm UV light irradiation.

Table S4. Determination of Ag^+ in water samples.

Sample	Ag^+ added (μmol/L)	Ag^+ found (μmol/L)	Recovery (%)	R.S.D. (n = 3) (%)
Tap water	0.1	0.109	109	1.26
	10	10.471	104.71	1.52
River water	0.1	0.097	97	2.33
	10	10.508	105.08	1.92

Notes and references

1 X. Cui, N. Vasylieva, P. Wu, B. Barnych, J. Yang, D. Shen, Q. He, S. J. Gee, S. Zhao and B. D. Hammock, *Anal. Chem.*, 2017, **89**, 11091–11097.

2 D. Shen, J. Zheng, X. Cui, Y. Chen, Q. He, R. Lv, Z. Li and S. Zhao, *Sens. Actuators B Chem.*, 2018, **256**, 846–852.

3 J. Qi, L. Xiao, Q. Zhang, J. Feng, G. Wang and J. Gong, *Biotechnol. Appl. Biochem.*, 2019, **66**, 591–596.

4 M. N. Yang, Y. F. Zhang, G. Y. Zhi, X. F. Gu, L. Han and D. H. Zhang, *Biotechnol. Appl. Biochem.*, 2020, **67**, 257–264.